Published in final edited form as:
Stem Cells. 2010 August ; 28(8): 1435–1445. doi:10.1002/stem.467.

Epithelial-mesenchymal transition-derived cells exhibit multi-lineage differentiation potential similar to mesenchymal stem cells

Venkata L. Battula[1], **Kurt W. Evans**[2], **Brett G. Hollier**[2], **Yuexi Shi**[1], **Frank C. Marini**[1], **Ayyakkannu Ayyanan**[3], **Rui-Yu Wang**[1], **Cathrin Brisken**[3], **Rudy Guerra**[4], **Michael Andreeff**[1,#], and **Sendurai A. Mani**[2,#]

[1]Section of Molecular Hematology and Therapy, Department of Stem Cell Transplantation and Cellular Therapy, The University of Texas-M.D. Anderson Cancer Center, Houston, Texas, USA [2]Department of Molecular Pathology, The University of Texas-M.D. Anderson Cancer Center, Houston, Texas, USA [3]ISREC, School of Life Science, Ecole Polytechnique Fédérale (EPFL), CH-1015 Lausanne, Switzerland [4]Department of Statistics, Rice University, Houston, Texas, USA

Summary

The epithelial-to-mesenchymal transition (EMT) is an embryonic process that becomes latent in most normal adult tissues. Recently, we have shown that induction of EMT endows breast epithelial cells with stem cell traits. In this report, we have further characterized the EMT-derived cells and shown that these cells are similar to mesenchymal stem cells (MSCs) with the capacity to differentiate into multiple tissue lineages. For this purpose, we induced EMT by ectopic expression of Twist, Snail or TGF-β in immortalized human mammary epithelial cells (HMECs). We found that the EMT-derived cells and MSCs share many properties including the antigenic profile typical of MSCs, i.e. $CD44^+$, $CD24^-$ and $CD45^-$. Conversely, MSCs express EMT-associated genes, such as Twist, Snail and FOXC2. Interestingly, CD140b (PDGFR-β), a marker for naive MSCs, is exclusively expressed in EMT-derived cells and not in their epithelial counterparts. Moreover, functional analyses revealed that EMT-derived cells but not the control cells can differentiate into Alizarin Red S-positive mature osteoblasts, Oil Red O-positive adipocytes and Alcian Blue-positive chondrocytes similar to MSCs. We also observed that EMT-derived cells but not the control cells invade and migrate towards MDA-MB-231 breast cancer cells similar to MSCs. *In vivo* wound homing assays in nude mice revealed that the EMT-derived cells home to wound sites similar to MSCs. In conclusion, we have demonstrated that the EMT-derived cells are similar to MSCs in gene expression, multi-lineage differentiation, and ability to migrate towards tumor cells and wound sites.

[#]Corresponding authors: Sendurai A. Mani PhD, 1515 Holcombe Blvd, Box: 0951, Houston, TX, 77030, Phone: 1- 713-792-9638, FAX: 1-713-834-6082, mani@mdanderson.org.

Author contribution:
VLB: Conception and design, collection and assembly of data, data analysis and interpretation, manuscript writing; KE: Collection and assembly of data, data analysis and interpretation, manuscript writing; BGH: Collection and assembly of data; YS: Collection and assembly of data; FCM: Collection and assembly of data, provision of study material; AA: Collection and assembly of data, Provision of study material; RW: Collection and assembly of data, provision of study material CB: provision of study material; MA: Conception and design, data analysis and interpretation, financial support, final approval of the manuscript; SAM: Conception and design, data analysis and interpretation, financial support, manuscript writing, final approval of the manuscript

DISCLOSURE OF POTENTIAL CONFLICTS OF INTEREST: S.A.M., K.W.E., V.L.B., and M.A. are inventors of a patent application in part based on findings described in this manuscript. The other authors have no financial interests to disclose.

Keywords

Epithelial-mesenchymal transition; Twist; Snail; MSC; mesenchymal stem cells; CD140b; PDGFR-beta

Introduction

Epithelial-to-mesenchymal transition (EMT) is a latent embryonic process that causes epithelial cells to lose their epithelial traits and acquire properties of mesenchymal cells. During EMT, epithelial cells lose cell polarity by downregulating the expression of cytokeratins and cell-cell adhesion molecules such as E-cadherin [1, 2]. The decrease in epithelial gene expression is accompanied by increased expression of mesenchymal genes, including vimentin and fibronectin. Following passage through EMT, epithelial cells also acquire a mesenchymal morphology in adherent culture and increased motility and invasiveness [1, 3, 4]. The EMT program plays an important role during the morphogenesis of multicellular organisms. For example, during gastrulation, epithelial cells located in the primitive streak undergo EMT followed by ingression and migration to a new location where they form endodermal and mesodermal embryonic tissues. In the absence of the EMT process, gastrulation does not occur and embryonic development does not progress past the blastula stage [5]. Similarly, during neural crest development, epithelial-looking cells within the neural plate shed their epithelial traits and gain a mesenchymal phenotype via EMT [6].

EMT can be induced by several cytokines and chemokines, including transforming growth factor-β (TGF-β), or by the expression of several developmentally-important transcription factors, including Twist and Snail [7, 8]. We recently demonstrated that induction of EMT by TGF-β1, Snail or Twist in immortalized human mammary epithelial cells results in the acquisition of stem cell characteristics [9]. These characteristics include the ability to form spheres in non-adherent culture [10] and a shift from the more differentiated mammary epithelial cell surface marker profile ($CD44^{low}CD24^{high}$) to the antigenic phenotype associated with mammary stem cells ($CD44^{high}CD24^{low}$) [9, 11]. However, these studies only began to delineate the molecular similarities between EMT-derived cells and stem cell populations and did not address the full lineage differentiation potential acquired by EMT-derived cells.

Mesenchymal stem cells (MSCs) are a small population of cells within the mesenchymal stromal cell compartment that have the capacity to self-renew and differentiate into multiple cell lineages including three major mesodermal lineages: osteoblasts, adipocytes and chondrocytes [12–14]. MSCs have been identified and propagated from various adult and fetal tissues including the bone marrow, adipose tissue, umbilical cord, human term placenta and endometrium [15–19]. MSCs express a panel of cell surface antigens, including CD105 (Endoglin), CD73 (Ecto-5'-nucleotidase), CD44 (Hyaluronic acid receptor), CD140b (PDGFR-β), CD90 (Thy-1), and are negative for markers of the hematopoietic lineage e.g. CD45 [20–23]. In addition, MSCs have been shown to engraft into wounds and damaged tissues [24, 25].

Herein, we report that EMT-derived cells have a functional resemblance to MSCs derived from human bone marrow, including a similar antigenic phenotype, the ability to differentiate into multiple cell lineages, and the potential to home to tumor cells *in vitro* and wounds *in vivo*.

Methods

Isolation and culture of primary MSCs

MSCs were isolated from the bone marrow of healthy donors who were undergoing bone marrow harvest for use in allogeneic bone marrow transplantation. All bone marrow donors provided written informed consent, and this study was conducted according to institutional guidelines under an approved protocol. Bone marrow was subjected to centrifugation (700×*g* for 15 minutes at 4 °C) over a Ficoll–Hypaque gradient (Sigma, St. Louis, MO) to separate mononuclear cells. After centrifugation, the buffy coat layer was carefully extracted and resuspended in alpha-minimal essential medium containing 20% fetal bovine serum (Gibco BRL, Rockville, MD), L-glutamine, and penicillin–streptomycin (Flow Laboratories, Rockville, MD) and plated at an initial density of 1×10^6 cells/cm^2. After three days, the cultures were washed with phosphate-buffered saline (PBS), and the remaining adherent cells were cultured until ~80% confluence. The cells were then subcultured at densities of 5000–6000 cells/cm^2. The third or fourth passage was used for the experiments.

Human mammary epithelial cell (HMECs) culture and generation of EMT-derived cells

The HMECs were transduced and maintained as previously described [9, 26]. In brief, HMECs obtained from Clonetics® were immortalized with the catalytic subunit of human telomerase and SV40 Large T antigen. These cells were then transduced with either pBabe-puro retroviral vector or pBabe-puro vectors expressing Twist, Snail, or TGF-β1. Bright field photographs were taken with a Nikon Coolpix 950 camera attached to a Nikon TMS light microscope (Nikon Instruments Inc., Melville, NY). Isolation, culturing and infection of primary human mammary epithelial cells are described in Ayyanan et al. 2006 [27].

RT-PCR analysis

Total RNA extraction and real-time RT-PCR were performed as previously reported [9] using ABI7900 real-time PCR machine. The primer sets used for detection of EMT-associated genes were previously described [9]. The primers used in the differentiation studies are listed in Supplementary Table 1.

Flow-cytometry

HMECs stably expressing *Twist*, *Snail, TGF-B1 or empty vector* or MSCs were trypsinized, washed once with PBS, once with PBS containing 4% FBS (FACS buffer), and then incubated in FACS buffer for 15 min on ice. Live cells (5×10^5) were then incubated with 1 μg of fluorochrome-conjugated antibodies in 100 μl reaction volume for 15 min. The following antibody conjugates were used: CD44-APC, CD90-PE, CD105-PE (eBiosciences San Diego, CA) and CD10-PE, CD11c-PE, CD14-PE, CD-24-FITC, CD45-FITC, CD73-PE, CD106-PE, CD140b-PE, CD166-PE (BD Bioscience San Jose, CA). After incubation, the cells were washed with FACS buffer containing 0.5μg/ml DAPI and analyzed on a LSR-II Flow Cytometer (BD Biosciences). Ten thousand events were acquired for each sample. The flow-cytometric data analysis was performed using FCS Express software (Denovo software, Los Angeles, CA).

Multilineage Differentiation

Osteoblast Differentiation—Ten thousand HMECs expressing the empty vector, Twist or Snail as well as MSCs were cultured in NH OsteoDiff® (Miltenyi Biotec, Auburn, CA) media for 21 days. The medium was replaced every 3 days. After 21 days, the cells were washed twice with PBS and fixed with 4% paraformaldehyde (PFA). To determine alkaline phosphatase activity, cells were incubated with FAST™ BCIP/NBT substrate (Sigma-Aldrich) for 20 min at room temperature. Calcium deposition was analyzed by staining with

1% Alizarin Red S (Spectrum®, Gardena, CA) for 5 min at room temperature. Mineral deposition was determined by Von-Kossa staining, which was performed by incubating fixed cells with 1% silver nitrate (Sigma-Aldrich) under bright light at room temperature for 30 min. For the gene expression analysis during osteoblast differentiation, total mRNA was collected from cells which were grown in osteoblast differentiation medium for either 0, 5, or 10 days during the course of differentiation. Real-time RT-PCR was performed on these samples as described above for alkaline phosphatase and osteocalcin using the primers described in Supplementary Table-1.

Adipocyte Differentiation—To test differentiation into adipocytes, the respective cells types were cultured in NH AdipoDiff® medium (Miltenyi Biotec). In brief, 2×10^4 of HMECs expressing the empty vector, Twist or Snail as well as MSCs were cultured in NH AdipoDiff® medium in a 12-well cell culture dish. The medium was replaced every 3 days. After 28 days of culture, the formation of adipocytes was evaluated fixing cells with 4% PFA and staining with Oil Red O dye (Sigma-Aldrich) for 15 min at RT. Alternatively, oil droplets were also stained using LipidTox®, a fluorescent lipid dye from Invitrogen. Photographs were taken either by using a Nikon Coolpix 950 camera attached to Nikon TMS light microscope (Nikon Instruments Inc.) or by Hamamatsu-C4742-95 camera (Hamamtsu, Bridgewater, NJ, USA) attached to Olympus IX-51 inverted fluorescent microscope (Olympus America Inc, Center Valley, PA). For the gene expression analysis during adipocyte differentiation, total mRNA was collected from cells which were grown in adipocyte differentiation medium for either 0, 5, or 10 days during the course of differentiation. Real-time RT-PCR was performed on these samples as described above for PPAR-gamma and lipoprotein lipase (LPL) using the primers described in Supplementary Table-1.

Chondrogenic differentiation—To induce differentiation into the chondrocyte lineage, the cells were incubated in ChondroDiff® medium (Miltenyi Biotec). Briefly, 4×10^5 of HMECs expressing the empty vector, Twist or Snail as well as MSCs were washed once with PBS and the cell pellets were cultured in 1 ml of ChodroDiff® medium in 15 ml falcon tubes for 21 days at 37°C. The medium was replaced every 3 days. After incubation, the resulting cell pellets were fixed with 3.7% formalin, embedded in paraffin, and cut into 5 μm thick sections. Following deparaffinization and hydratation, the sections were incubated with Alcian Blue 8GX solution (Sigma-Aldrich) for 30 min at room temperature. The slides were then washed in 3% acetic acid and then in distilled water. After washing, the slides were counter stained with nuclear fast Red (Sigma) for 5 minutes and then washed with distilled water. Photographs were taken using Hamamatsu-C4742-95 camera (Hamamatsu) attached to Olympus BX41 microscope (Olympus America Inc).

Alternatively, the sections were immune-stained with collagen-I or collagen-II antibody (Abcam, Cambridge, MA) as described earlier using paraffin-embedded tissue sections [28]. Briefly, after blocking with specific blocking buffer (Dako, Carpinteria, CA), the sections were then incubated with rabbit anti-human collagen-I or collagen-II polyclonal antibody (Abcam) overnight at 4°C. The sections were washed three times with PBST and then incubated with biotinylated secondary antibody and HRP-conjugated streptavidin complex, as described in the manufacturer's instructions (Dako). After washing the sections with wash buffer, the staining was visualized using 3,3'-diaminobenzidine (DAB). The pictures were taken with Olympus DP-70 camera attached to Olympus BX-41 microscope (Olympus America Inc.)

Wound homing assay

Luciferase labeling using adenoviral vector transduction—A recombinant adenoviral (Ad) vector expressing firefly luciferase (ffLuc) and possessing an RGD-modified fiber (AdLuc-F/RGD) was prepared, purified, and tittered as previously described [29]. HMECs expressing the empty vector, Twist or Snail as well as MSCs were incubated for 4 hours, in serum-free medium with 2,000 AdLuc-F/RGD viral particles per cell. The transduced cells were assessed for luciferase expression by plating 5×10^4 cells into 24 well plates and adding 40 μg of D-Luciferin (Caliper Life Sciences, Hopkinton, MA) into 2 ml culture medium. After 30 s, the cells were placed into the imager for detection. Using this multiplicity of infection (MOI) protocol, we routinely detected >500 copies of Ad-delivered ffLuc transcript/cell by qRT-PCR, and bioluminescence could be detected for up to 30 days (data not shown).

In vivo wound homing model in nude mice—Nude mice (NU/J, The Jackson laboratory, Bar Harbor, Maine, USA) were housed according to institutional standards and treated with approved protocols. To generate the wounding model, mice were first anesthetized and then 4 mm diameter punch biopsies were made on the dorsal side of the animals using Biopsy Punch (4.0 mm, HealthLink, http://healthlinkinc.net/). To analyze the wound homing ability, 3×10^5 luciferase-labeled cells were transplanted through the tail vain on the day of wounding. The mice were imaged after 3 days as described below. All mouse work was performed following institutional-approved protocols.

Bioluminescent in-vivo imaging—*In vivo* optical imaging was performed with a Xenogen IVIS bioluminescence/fluorescence optical imaging system (Caliper Life Sciences [Xenogen], Hopkinton, MA). Five minutes prior to imaging, each mouse was given an intraperitoneal injection of D-luciferin (at a dose of 125 mg/kg or a 100 Rl injection of 40 mg/ml coelenterazine) as described previously. General anesthesia was given (5% isoflurane [IsoSol, Medeva Pharmaceutical PA, Inc.]), and the mice were placed in the light-tight heated chamber. Anterior and posterior luminescent images were acquired with 1- to 3-minute exposure times. Optical images were displayed and analyzed with IVIS Living Image (Caliper Life Sciences [Xenogen], Hopkinton, MA) software packages.

In vitro Matrigel invasion assay

An *in vitro* Matrigel invasion assay was performed using 24-well Biocoat Matrigel Invasion Chambers containing BD Falcon™ Cell Culture Inserts with 8 micron diameter pore size PET membrane that has been treated with Matirgel Matrix (BD Biosciences). The MSCs were serum-starved for 24hr before the assay to avoid any receptor blocking factors from serum. There was no such treatment for HMEC cells, as they are cultured in serum free medium. In addition, 5×10^4 MDA-MB-231 cells were plated into 24-well cell culture dishes. To perform the assay, at first the inserts containing Matrigel were hydrated using 500 μl of warm culture medium without serum at 37°C for 2h. After hydration, the medium was removed from the chambers and the inserts were placed on top of each well of the MDA-MB-231 cell containing culture dish. In case of PDGF-bb mediated invasion assays, medium in the bottom chamber was replaced with fresh medium with/without 10ng/ml PDGF-bb ligand (Peprotech, Rocky Hill, NJ, USA). Cell suspensions of vector, Twist or Snail over-expressing HMEC or MSCs were adjusted to a concentration of 15×10^4 cells/ml and, and 200μl of the adjusted cell suspension (3×10^4 cells/insert) was immediately placed in the Matrigel-coated upper chamber. After incubation at 37°C for 36h in a 5% CO2 incubator, the residual cells on the upper surface of the filter were completely removed with cotton swabs. The membranes were then stained with HEMA-3® hematoxylin solution (Fisher scientific company L.L.C., Kalamazoo, MI), and the invasive potential of the cells was determined by counting the number of cells that had invaded to the lower surface of the

filter in 10 different areas under a inverted light microscope (Olympus BX41). Each assay was performed in triplicate in 3 separate experiments.

Gene chip data Analysis and Statistical Methods

Gene chip analysis was performed in triplicate to compare the gene expression changes between the HMECs expressing the control vector, or Snail, with that of MSCs. Prior to statistical analysis of gene expression probe sets were matched between the two generations of Affymetrix chips, HT_HG_U133A and HG_U133_Plus_2. The former chip is a subset of the latter chip and, therefore, the analysis of differential expression was restricted to the probe sets on the HT_HG_U133A chip. Probe sets between the HT_HG_U133A chip and the HG_U133_Plus_2 chip were matched using the function read.affybatch.hybrid from the CustomCDF R package [30]. A total of 22,268 probesets representing 13,294 genes were matched and analyzed.

The statistical analysis of the Affymetrix CEL data was performed using the Bioconductor [31] statistical software environment. To assess differential expression, the intensity values in the CEL files were transformed to RMA (Robust Multichip Average) expression measures [32]. The RMA measure is given in a log base 2 scale. Using the Limma R package, we fit linear models with the lmFit function to simultaneously assess pair wise differential expression among the three RNA sources.

Results

Comparison of EMT-derived cells with MSCs

Given that MSCs have mesenchymal features, including morphology (Figure 1A), and exhibit stem cell characteristics [14], we sought to determine whether epithelial cells that have undergone EMT share molecular and functional properties with MSCs. We first determined whether HMECs stably expressing Twist, Snail or TGF-β1 exhibited properties of MSCs by analyzing the expression of several cell surface markers associated with MSCs in EMT-derived HMECs using flow cytometry. We found that EMT-derived cells expressed several MSCs-associated cell surface markers including, CD10, CD44, CD73, CD90, CD105, CD106 and CD166 (Table 1). Interestingly, CD140b (Platelet Derived Growth Factor Receptor β [PDGFR-β]), a prospective marker for isolation of MSCs from human bone-marrow [21], was highly expressed on the surface of EMT-derived HMECs but not on the vector control HMECs (Figure 1D). Importantly, both the EMT-derived HMECs and MSCs were negative for CD45, CD11c and CD14, which are hematopoietic lineage markers (Figure 1D, Table 1). These findings suggested that mesenchymal-like cells generated from HMECs by EMT and MSCs express a similar set of cell surface antigens.

Since EMT-derived HMECs exhibited a similar antigenic profile to MSCs, we determined whether MSCs obtained from human bone marrow express the mRNAs encoding markers associated with the mesenchymal-like state generated by EMT. During EMT, epithelial cells lose expression of E-cadherin and gain expression of mesenchymal-associated genes, such as N-cadherin, fibronectin and vimentin [33]. Most importantly, we found that the MSCs also expressed lower levels of E-cadherin and higher levels of vimentin, fibronectin, and N-cadherin compared to control epithelial cells (Figure 1B) [9]. Strikingly, the MSCs expressed high levels of embryonic transcription factors known to regulate EMT (i.e. Snail, Twist, Mesenchyme Forkhead 1 [FOXC2], Zeb1) (Figure 1C). Compared to HMECs, the MSCs also expressed high levels of CD44 and low levels of CD24 at the cell surface, which was similar to the EMT-derived stem-like cells (Figure 1D).

Global gene expression analysis, using Affymetirx microarrays, revealed that the sets of genes differentially expressed between vector-control HMECs and either MSCs or Snail-

induced EMT-derived HMECs were ~70% similar. On the other hand, 15% of the genes analyzed were differentially expressed between MSCs and Snail-induced EMT-derived HMECs. For example, several cytokeratins are more highly expressed in EMT-derived cells compared to MSCs (Supplementary Figure 1B, Supplemental File 1 & 2), which indicated that MSCs and EMT-derived cells have highly similar gene expression compared to the epithelial control cells but that the Snail-induced HMECs still maintain some characteristics of their epithelial origin.

Differentiation of EMT-derived cells into mesodermal lineages

Since the EMT-derived HMECs and MSCs had similar cell surface marker profiles, morphologies, and gene expression profiles, we next investigated whether EMT-derived HMECs have MSCs-like multipotency including the ability to differentiate into osteoblasts, adipocytes and chondrocytes. To test this, we first subjected the EMT-derived HMECs (Twist-/Snail-induced), along with vector-infected control epithelial cells, to an osteoblast differentiation assay. After 21 days, the cells were stained with FASTÔ BCIP/NBT substrate to analyze for alkaline phosphatase activity. Strikingly, the epithelial cells that had undergone EMT stained positive for alkaline phosphatase, a marker of osteoblasts (Figure 2A, left panel), similar to MSCs isolated from human bone marrow (Figure 2A, right panel). Furthermore, both Snail and Twist-induced, EMT-derived cells displayed a gradual increase alkaline phosphatase activity, in a time dependent manner, from week 1 to 3 of osteoblast differentiation culture (Supplementary Figure 2).

To further test if the EMT-derived cells could differentiate into functional osteoblasts capable of producing mineral deposits, cells were grown in osteoblast differentiation media and then stained with either 1% Alizarin Red S or 2% silver nitrate (von Kossa staining), which stains calcium deposits. The EMT-derived cells stained positive for Alizarin Red S and von Kossa reagent in a fashion comparable to bone marrow-derived MSCs (Figure 2 B & C). These findings showed that the EMT-derived cells produce calcium in response to differentiation conditions similar to MSCs. However, both the vector-control cells that were subjected to differentiation condition (Figure 2 B & C) and the EMT-derived cells that were not subjected to osteogenic differentiation were not capable of producing calcium (Supplemental Figure 3A). In addition, subjecting EMT-derived cells to an osteoblast differentiation assay increased the levels of mRNAs encoding osteoblast related genes, osteocalcin (OC) (Fold Change: Snail, 3.69; Twist, 11.11) and alkaline phosphatase (AP) (Fold Change: Snail, 9.39; Twist, 1.03) after 5 days in the differentiation condition (Figure 2D). These gene expression changes were maintained from day 5 to day 10. Under the identical conditions, there were no significant changes in the expression of these genes in vector-control cells. Together, these findings indicated that mesenchymal-like cells generated by EMT have the potential to differentiate into mature osteoblasts similar to MSCs.

Since MSCs are capable of differentiating into adipocytes [34], we next tested whether the mesenchymal-like cells generated by EMT could be differentiated into adipocytes. For this, we cultured EMT-derived cells in adipocyte differentiation media for 28 days and then stained the cultures for the presence of lipid droplets, a characteristic of mature adipocytes, using either Oil Red O dye (Figure 3A top panel) or the fluorescent LipidTox® dye (Figure 3A bottom panel). Indeed, the mesenchymal-like cells generated by EMT were capable of differentiating into adipocytes (Figure 3A) similar to MSCs isolated from human bone marrow (Figure 3A right panel). In contrast, the vector-transduced epithelial control cells did not differentiate into adipocytes under the same conditions (Figure 3A left panel). The EMT-derived cells subjected to adipocyte differentiation expressed higher levels of PPARγ (up to 10 fold, Figure 3B) upon differentiation relative to the undifferentiated cells. In addition, after 5 days in differentiation culture, lipoprotein lipase (LPL), a gene that is

involved in differentiation of adipocytes, was upregulated 9.74- and 16.88-fold in Twist- and Snail-induced cells, respectively, and this was further increased to 25.41- and 27.68-fold, respectively, after 10 days (Figure 3C). We observed a slight increase in LPL expression in the vector control cells at day 10 but to a lesser extent than EMT-derived cells and MSCs. Importantly, the parental EMT-derived cells did not stain positive for adipocytes differentiation markers prior to adipocyte differentiation culture (Supplementary Figure 3B). This evidence suggested that EMT-derived mesenchymal-like cells have the potential to differentiate into adipocytes.

Another well-known property of MSCs is the ability to differentiate into chondrocytes, which are the specialized cells in cartilage tissues that produce and maintain the collagen and proteoglycan [35]. To test whether EMT-derived cells can differentiate into chondrocytes, we cultured the cells that had undergone EMT due to ectopic expression of Twist or Snail in chondrocyte differentiation medium. After 21 days in suspension culture, the EMT-derived HMECs formed chondrocyte nodules similar to MSCs. In contrast, the vector-control cells did not form any chondrocyte nodules under identical culture conditions. To further confirm chondrocyte differentiation, we fixed, sectioned, and stained the chondrocyte nodules with Alcian Blue reagent in order to detect acid mucous substances and acetic mucins. We found that these nodules stained positive for alcian blue (Figure 3D, top panel), which revealed that the EMT-derived HMECs can differentiate into chondrocytes. Furthermore, the chondrocytes derived from EMT-derived cells and MSCs were positive for collagen I (Figure 3D, middle panel), and weakly positive for collagen II (Figure 3D, bottom panel). Together, these findings indicate that the mesenchymal-like cells generated by EMT are multipotent and have the potential to differentiate into the three major mesodermal lineages.

Invasion of EMT-derived cells towards PDGF-bb

Both MSCs and EMT-derived cells express PDGFR-β (Figure 1D), and studies have found that MSCs invade towards PDGF-bb [36]. In addition, we have reported that inducing EMT enhances the invasion potential of the transformed cells [8]. Therefore, we determined the ability of EMT-derived cells to invade towards PDGF-bb ligand. For this, we performed a chemotaxis assay by placing either EMT-derived cells or MSCs in the upper chamber and PDGF-bb in the bottom chamber (Figure 4A). We found that the EMT-derived HMECs (Twist-/Snail-induced) invaded towards PDGF-bb in comparison to the untreated cells. The level of invasion was similar to that observed by MSCs (Figure 4B and Supplementary Figure 4A). In contrast, vector control cells did not invade towards PDGF-bb.

Invasion of EMT-derived cells towards tumor cells

Bone marrow-derived MSCs have been shown home to tumor sites [37–39]. Since EMT-derived cells behaved similar to MSCs in respect to their multipotency, we tested whether EMT-derived cells also invaded towards tumor cells *in vitro*. For this, we performed a matrigel invasion assay by placing the EMT-derived HMECs (Twist-/Snail-induced) or MSCs in the upper chamber and MDA-MB-231 breast cancer cells in the bottom chamber (Figure 4A). Interestingly, we found that the EMT-derived HMECs invaded towards MDA-MB-231 6-fold more than did the control cells (Figure 4C and Supplementary Figure 4B).

Homing of EMT-derived cells into wounds *in vivo*

MSCs are shown to possess an intrinsic ability to home to damaged tissues and tumor sites [38, 40]. Since we found that the MSCs and EMT-derived cells migrate efficiently towards PDGF, we also examined their ability to home to wounded tissues *in vivo*. For this purpose, we injected luciferase-labeled EMT-derived cells, control cells and MSCs into the tail vein of nude mice bearing dorsal wounds. After three days, the animals were analyzed using

bioluminescent whole-animal imaging. Interestingly, the luciferase-labeled EMT-derived cells and the bone marrow-derived MSCs were detected specifically in the region of the wound (Figure 5A). In contrast, only a few vector control cells were detected in the wounded area (Figure 5A). Quantification of the photon counts at the wound site revealed a 6–7 fold increase in photons at the wound site by both EMT-derived cell populations (Twist 7+/−SD, Snail 6+/− SD) and MSCs (6+/− SD) as compared to vector control cells, (Figure 5B). These results indicate that the EMT-derived cells home to wounds similar to MSCs.

Discussion

The evidence presented here shows for the first time that EMT-derived cells have MSC-like multipotency. However, the current evidence is not sufficient to conclude the full spectrum of differentiation potential conferred by EMT. Therefore, further work is necessary to determine if EMT-derived cells can also differentiate into ectodermal, endodermal and other mesodermal lineages, including astrocytes, oligodendrocytes and cardiomyocytes, as previously demonstrated for MSCs [41–43].

Currently, there is a strong need for adult stem cells to be used in regenerative medicine, which is further extended due to concerns with embryonic stem cells. This is especially true for diseases such as osteoporosis and osteoarthritis. In these diseases, there is a hope that stem cell-based therapies can replace the vanished bone or cartilage. Here, we provided evidence that EMT-derived cells are multi-potent and can be differentiated into mature osteoblasts and chondrocytes. This suggests that future studies may consider using this cellular process, i.e. EMT, in the development of therapeutics aimed at the regeneration of damaged tissues. Possibly, epithelium from patients could be collected, induced to undergo EMT and then transplanted into the injured site of the same patient. This could possibly eliminate the influence of HLA-mismatch on graft rejection.

As epithelial tissues are highly abundant and more easily accessible than the bone marrow, it is possible that the laborious process of bone marrow collection could be avoided. In addition, isolating homogenous populations of MSCs is not easy. First, MSCs are a very small portion of the total human bone marrow according to the colony forming (CFU-f) assays (only 0.01%) [15]. Second, a perfect combination of cell surface markers is not available to isolate a completely homogenous population of MSCs. Currently, MSCs are isolated using either single or combination of cell surface markers, including STRO-1, CD271, MSCA-1, CD73, CD105, CD140b, and GD2. The alternative method of isolating MSCs by culturing the un-fractionated bone marrow samples in vitro and collecting the adherent populations after a few passages also does not provide a homogenous population. Our data suggest that, after extensive analysis and continued careful research, it may be possible to obtain more homogenous population of MSC-like cells for clinical use by inducing homogenous population of epithelial cells to undergo transient EMT.

In the context of tumor pathogenesis, EMT can promote cancer progression [44, 45]. Our findings suggest that EMT-derived cells may promote the metastasis of other tumor cells in a fashion similar to that suggested for MSCs [46]. Our findings also suggest that EMT-derived cells may be more capable of adapting to the environment encountered at the site of dissemination via (1) generation of a pre-survival/pro-expansion niche and/or (2) themselves adapting directly. In addition, the ability of EMT-derived cells to home to wounds in a manner similar to MSCs suggests that EMT generates cells with both the motility to disseminate and the plasticity [47] needed to adapt to a foreign environment. Moreover, through the EMT process, normal or cancerous cells may acquire multipotency, migrate to wounded tissues, and depending on the nature of the cell, either repair damaged tissues or seed a tumor. Even though, we observed varying degrees of differentiation into osteoblasts,

adipocytes and chondrocytes by Twist or Snail expressing HMECs, they both differentiated into all three lineages. For example, we observed Snail-expressing HMECs differentiate better into adipocyte than the twist-expressing HMECs. Although, there is an increase in the number of osteoblasts generated in the Twist expressing HMECs compared to Snail expressing HMECs in Supplementary figure 2, it is because of differences in cells proliferation but not because of Twist expressing cells produces more differentiated cells than Snail expressing cells. Twist expressing HMECs proliferate twice as fast as Snail expressing HMECs (data not shown).

The homing capacity of MSCs to wounds and tumors [24, 25, 40] has led to studies exploring the utility of MSCs as anti-tumor cellular delivery vehicles [38, 39]. Our previous findings suggest that intravenous delivery of MSCs may be a less invasive option for stem cell-based therapeutic techniques [38, 39]. Since EMT-derived cells and MSCs share a similar intrinsic ability to home to wounds, EMT-derived cells may also be useful in stem cell-based drug delivery.

Finally, our findings of induction of PDGFR during EMT and invasion of EMT-derived cells towards PDGF-bb similar to MSCs suggest that PDGF mediated signaling might be important for the migration of EMT-derived cells *in vivo*. In addition, previous reports [48, 49] also support this idea by showing that treating wounds with recombinant PDGF enhances wound healing in healthy individuals. Our findings suggest this effect may be mediated by the recruitment of both MSCs and EMT-derived cells from the near proximity via PDGF-mediated signaling.

Conclusion

Collectively, these findings indicate that EMT-derived cells not only express markers that are relevant to MSCs but also exhibit functional similarities to MSCs. These EMT-derived cells are capable of differentiating into mature osteoblasts, adipocytes and chondrocytes similar to MSCs obtained from human bone marrow. Interestingly, EMT derived cells migrate towards wounds *in vivo* and to tumor cells *in vitro* similar to MSCs. In this report, we show, for the first time, that EMT-derived cells behaved functionally and phenotypically similar to MSCs, a subpopulation of adult stem cells.

Supplementary Material

Refer to Web version on PubMed Central for supplementary material.

Acknowledgments

We are grateful to Robert Weinberg for his support, reagents and critical reading of the manuscript. We thank Nathalie Sphyris, Joe Taube and Agata Tinnirello for critical reading of the manuscript and Sreedevi Kumar for the technical help. We are indebted to anonymous reviewers for their helpful suggestions, which improved the manuscript significantly. SAM is supported in part by the M. D. Anderson Cancer Center Research Trust and The V Foundation. FCM and MA are supported in part by grants from the National Cancer Institute (RC1CA146381, CA-109451 and CA-116199 to FCM, CA-55164, CA-16672, and CA-49639 for MA) and by the Paul and Mary Haas Chair in Genetics (MA).

References

1. Hay ED. An overview of epithelio-mesenchymal transformation. Acta Anat (Basel). 1995; 154:8–20. [PubMed: 8714286]
2. Kalluri R, Neilson EG. Epithelial-mesenchymal transition and its implications for fibrosis. J Clin Invest. 2003; 112:1776–1784. [PubMed: 14679171]

3. Shook D, Keller R. Mechanisms, mechanics and function of epithelial-mesenchymal transitions in early development. Mechanisms of development. 2003; 120:1351–1383. [PubMed: 14623443]
4. Thiery JP. Epithelial-mesenchymal transitions in development and pathologies. Current opinion in cell biology. 2003; 15:740–746. [PubMed: 14644200]
5. Thiery JP, Sleeman JP. Complex networks orchestrate epithelial-mesenchymal transitions. Nat Rev Mol Cell Biol. 2006; 7:131–142. [PubMed: 16493418]
6. Duband JL, Monier F, Delannet M, et al. Epithelium-mesenchyme transition during neural crest development. Acta Anat (Basel). 1995; 154:63–78. [PubMed: 8714290]
7. Nawshad A, LaGamba D, Hay ED. Transforming growth factor beta (TGFbeta) signalling in palatal growth, apoptosis and epithelial mesenchymal transformation (EMT). Archives of oral biology. 2004; 49:675–689. [PubMed: 15275855]
8. Yang J, Mani SA, Donaher JL, et al. Twist, a master regulator of morphogenesis, plays an essential role in tumor metastasis. Cell. 2004; 117:927–939. [PubMed: 15210113]
9. Mani SA, Guo W, Liao MJ, et al. The epithelial-mesenchymal transition generates cells with properties of stem cells. Cell. 2008; 133:704–715. [PubMed: 18485877]
10. Dontu G, Al-Hajj M, Abdallah WM, et al. Stem cells in normal breast development and breast cancer. Cell Prolif. 2003; 36(Suppl 1):59–72. [PubMed: 14521516]
11. Al-Hajj M, Wicha MS, Benito-Hernandez A, et al. Prospective identification of tumorigenic breast cancer cells. Proc Natl Acad Sci U S A. 2003; 100:3983–3988. [PubMed: 12629218]
12. Friedman MS, Long MW, Hankenson KD. Osteogenic differentiation of human mesenchymal stem cells is regulated by bone morphogenetic protein-6. Journal of cellular biochemistry. 2006; 98:538–554. [PubMed: 16317727]
13. in 't Anker PS, Noort WA, Scherjon SA, et al. Mesenchymal stem cells in human second-trimester bone marrow, liver, lung, and spleen exhibit a similar immunophenotype but a heterogeneous multilineage differentiation potential. Haematologica. 2003; 88:845–852. [PubMed: 12935972]
14. Short B, Brouard N, Occhiodoro-Scott T, et al. Mesenchymal stem cells. Archives of medical research. 2003; 34:565–571. [PubMed: 14734097]
15. Battula VL, Bareiss PM, Treml S, et al. Human placenta and bone marrow derived MSC cultured in serum-free, b-FGF-containing medium express cell surface frizzled-9 and SSEA-4 and give rise to multilineage differentiation. Differentiation; research in biological diversity. 2007; 75:279–291.
16. Erices A, Conget P, Minguell JJ. Mesenchymal progenitor cells in human umbilical cord blood. British journal of haematology. 2000; 109:235–242. [PubMed: 10848804]
17. Friedenstein AJ, Gorskaja JF, Kulagina NN. Fibroblast precursors in normal and irradiated mouse hematopoietic organs. Experimental hematology. 1976; 4:267–274. [PubMed: 976387]
18. Morizono K, De Ugarte DA, Zhu M, et al. Multilineage cells from adipose tissue as gene delivery vehicles. Hum Gene Ther. 2003; 14:59–66. [PubMed: 12573059]
19. Dimitrov R, Timeva T, Kyurkchiev D, et al. Characterization of clonogenic stromal cells isolated from human endometrium. Reproduction. 2008; 135:551–558. [PubMed: 18367513]
20. Battula VL, Treml S, Abele H, et al. Prospective isolation and characterization of mesenchymal stem cells from human placenta using a frizzled-9-specific monoclonal antibody. Differentiation; research in biological diversity. 2008; 76:326–336.
21. Buhring HJ, Battula VL, Treml S, et al. Novel markers for the prospective isolation of human MSC. Annals of the New York Academy of Sciences. 2007; 1106:262–271. [PubMed: 17395729]
22. Caplan AI. Mesenchymal stem cells. J Orthop Res. 1991; 9:641–650. [PubMed: 1870029]
23. Uccelli A, Moretta L, Pistoia V. Mesenchymal stem cells in health and disease. Nature reviews. 2008
24. Herdrich BJ, Lind RC, Liechty KW. Multipotent adult progenitor cells: their role in wound healing and the treatment of dermal wounds. Cytotherapy. 2008; 10:543–550. [PubMed: 18836914]
25. Spees JL, Whitney MJ, Sullivan DE, et al. Bone marrow progenitor cells contribute to repair and remodeling of the lung and heart in a rat model of progressive pulmonary hypertension. Faseb J. 2008; 22:1226–1236. [PubMed: 18032636]

26. Elenbaas B, Spirio L, Koerner F, et al. Human breast cancer cells generated by oncogenic transformation of primary mammary epithelial cells. Genes & development. 2001; 15:50–65. [PubMed: 11156605]
27. Ayyanan A, Civenni G, Ciarloni L, et al. Increased Wnt signaling triggers oncogenic conversion of human breast epithelial cells by a Notch-dependent mechanism. Proc Natl Acad Sci U S A. 2006; 103:3799–3804. [PubMed: 16501043]
28. Zeng Z, Shi YX, Samudio IJ, et al. Targeting the leukemia microenvironment by CXCR4 inhibition overcomes resistance to kinase inhibitors and chemotherapy in AML. Blood. 2009; 113:6215–6224. [PubMed: 18955566]
29. Klopp AH, Spaeth EL, Dembinski JL, et al. Tumor irradiation increases the recruitment of circulating mesenchymal stem cells into the tumor microenvironment. Cancer research. 2007; 67:11687–11695. [PubMed: 18089798]
30. Dai C, Liu J. Inducing Pairwise Gene Interactions from Time-Series Data by EDA Based Bayesian Network. Conf Proc IEEE Eng Med Biol Soc. 2005; 7:7746–7749. [PubMed: 17282077]
31. Huber W, Gentleman R. matchprobes: a Bioconductor package for the sequence-matching of microarray probe elements. Bioinformatics. 2004; 20:1651–1652. [PubMed: 14988118]
32. Irizarry RA, Ooi SL, Wu Z, et al. Use of mixture models in a microarray-based screening procedure for detecting differentially represented yeast mutants. Stat Appl Genet Mol Biol. 2003; 2 Article1.
33. Zeisberg M, Neilson EG. Biomarkers for epithelial-mesenchymal transitions. J Clin Invest. 2009; 119:1429–1437. [PubMed: 19487819]
34. Kolf CM, Cho E, Tuan RS. Mesenchymal stromal cells. Biology of adult mesenchymal stem cells: regulation of niche, self-renewal and differentiation. Arthritis research & therapy. 2007; 9:204. [PubMed: 17316462]
35. Mackay AM, Beck SC, Murphy JM, et al. Chondrogenic differentiation of cultured human mesenchymal stem cells from marrow. Tissue Eng. 1998; 4:415–428. [PubMed: 9916173]
36. Tokunaga A, Oya T, Ishii Y, et al. PDGF receptor beta is a potent regulator of mesenchymal stromal cell function. J Bone Miner Res. 2008; 23:1519–1528. [PubMed: 18410236]
37. Spaeth E, Klopp A, Dembinski J, et al. Inflammation and tumor microenvironments: defining the migratory itinerary of mesenchymal stem cells. Gene Ther. 2008; 15:730–738. [PubMed: 18401438]
38. Studeny M, Marini FC, Champlin RE, et al. Bone marrow-derived mesenchymal stem cells as vehicles for interferon-beta delivery into tumors. Cancer research. 2002; 62:3603–3608. [PubMed: 12097260]
39. Studeny M, Marini FC, Dembinski JL, et al. Mesenchymal stem cells: potential precursors for tumor stroma and targeted-delivery vehicles for anticancer agents. Journal of the National Cancer Institute. 2004; 96:1593–1603. [PubMed: 15523088]
40. Bittira B, Shum-Tim D, Al-Khaldi A, et al. Mobilization and homing of bone marrow stromal cells in myocardial infarction. Eur J Cardiothorac Surg. 2003; 24:393–398. [PubMed: 12965310]
41. Kopen GC, Prockop DJ, Phinney DG. Marrow stromal cells migrate throughout forebrain and cerebellum, and they differentiate into astrocytes after injection into neonatal mouse brains. Proc Natl Acad Sci U S A. 1999; 96:10711–10716. [PubMed: 10485891]
42. Neuhuber B, Gallo G, Howard L, et al. Reevaluation of in vitro differentiation protocols for bone marrow stromal cells: disruption of actin cytoskeleton induces rapid morphological changes and mimics neuronal phenotype. J Neurosci Res. 2004; 77:192–204. [PubMed: 15211586]
43. Quevedo HC, Hatzistergos KE, Oskouei BN, et al. Allogeneic mesenchymal stem cells restore cardiac function in chronic ischemic cardiomyopathy via trilineage differentiating capacity. Proc Natl Acad Sci U S A. 2009; 106:14022–14027. [PubMed: 19666564]
44. Janda E, Lehmann K, Killisch I, et al. Ras and TGF[beta] cooperatively regulate epithelial cell plasticity and metastasis: dissection of Ras signaling pathways. J Cell Biol. 2002; 156:299–313. [PubMed: 11790801]
45. Kiemer AK, Takeuchi K, Quinlan MP. Identification of genes involved in epithelial-mesenchymal transition and tumor progression. Oncogene. 2001; 20:6679–6688. [PubMed: 11709702]

46. Karnoub AE, Dash AB, Vo AP, et al. Mesenchymal stem cells within tumour stroma promote breast cancer metastasis. Nature. 2007; 449:557–563. [PubMed: 17914389]

47. Savagner P, Kusewitt DF, Carver EA, et al. Developmental transcription factor slug is required for effective re-epithelialization by adult keratinocytes. J Cell Physiol. 2005; 202:858–866. [PubMed: 15389643]

48. Bhattacharyya J, Mondal G, Madhusudana K, et al. Single subcutaneous administration of RGDK-lipopeptide:rhPDGF-B gene complex heals wounds in streptozotocin-induced diabetic rats. Mol Pharm. 2009; 6:918–927. [PubMed: 19388683]

49. Moore DC, Ehrlich MG, McAllister SC, et al. Recombinant human platelet-derived growth factor-BB augmentation of new-bone formation in a rat model of distraction osteogenesis. J Bone Joint Surg Am. 2009; 91:1973–1984. [PubMed: 19651957]

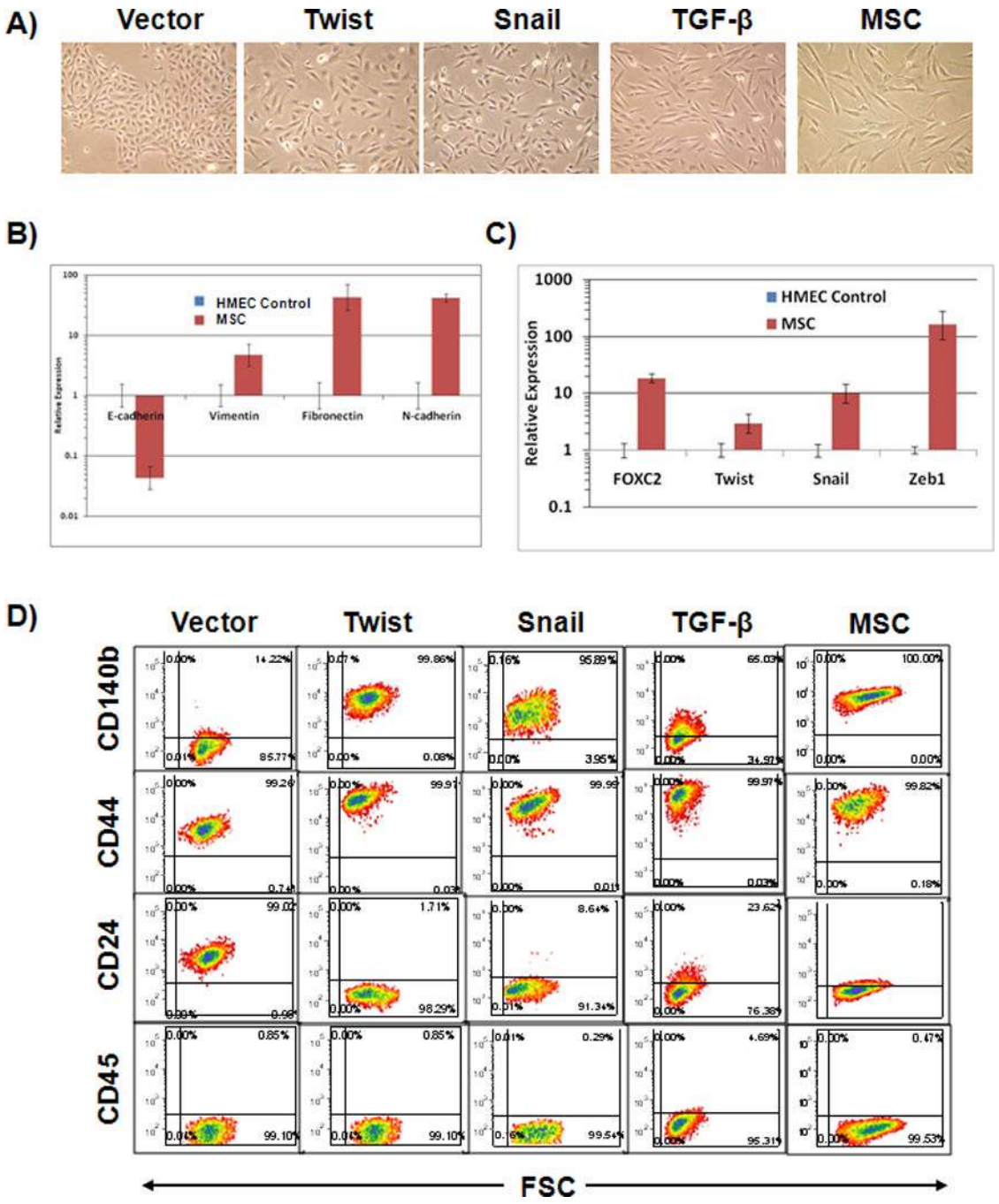

Figure 1.

Morphology and expression pattern of genes in EMT-derived HMECs and bone marrow MSCs. **A.** Light microscopic images (10X) of HMECs ectopically expressing Twist, Snail, TGF-β1 or the empty vector as well as bone marrow-derived MSCs. **B&C.** Quantitative RT-PCR analysis of EMT associated genes including E-cadherin, vimentin, fibronectin and N-cadherin (B) and EMT-regulating transcription factors, including FOXC2, Twist, Snail, and Zeb-1 in MSCs (C). **D.** The expression of cell surface markers associated with MSCs in EMT-derived HMECs expressing Twist, Snail, TGF-β or the control vector. Quantitative RT-PCR was performed in triplicate (mean +/− SD).

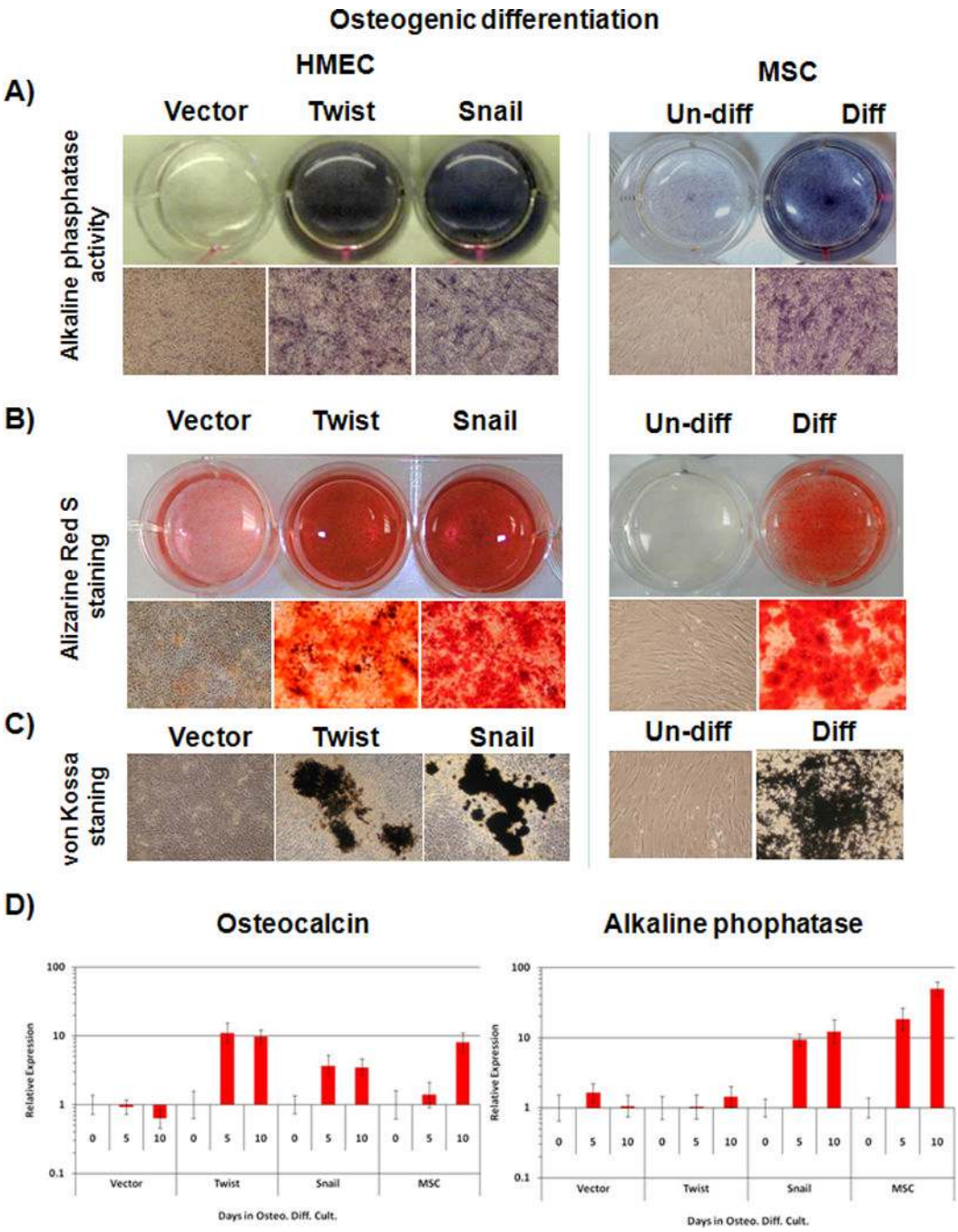

Figure 2.

Osteoblastic differentiation of EMT-derived mesenchyme-like HMECs and MSCs. **A**. Following culture in osteoblastic differentiation media, HMECs expressing Twist or Snail and MSCs were positive for alkaline phosphatase activity while the vector control cells were not. **B&C.** Staining for calcium deposition in EMT-derived HMECs and MSCs after osteoblastic differentiation using 1% Alizarin Red S (B) or 1% silver nitrate (von Kossa staining) (C). **D**. Quantitative RT-PCR analysis for the expression of osteoblast markers osteocalcin (left panel) and alkaline phosphatase (right panel) in EMT-derived HMECs,

control HMECs and MSCs subjected to osteoblast differentiation for different lengths of time (0, 5 and 10 days).

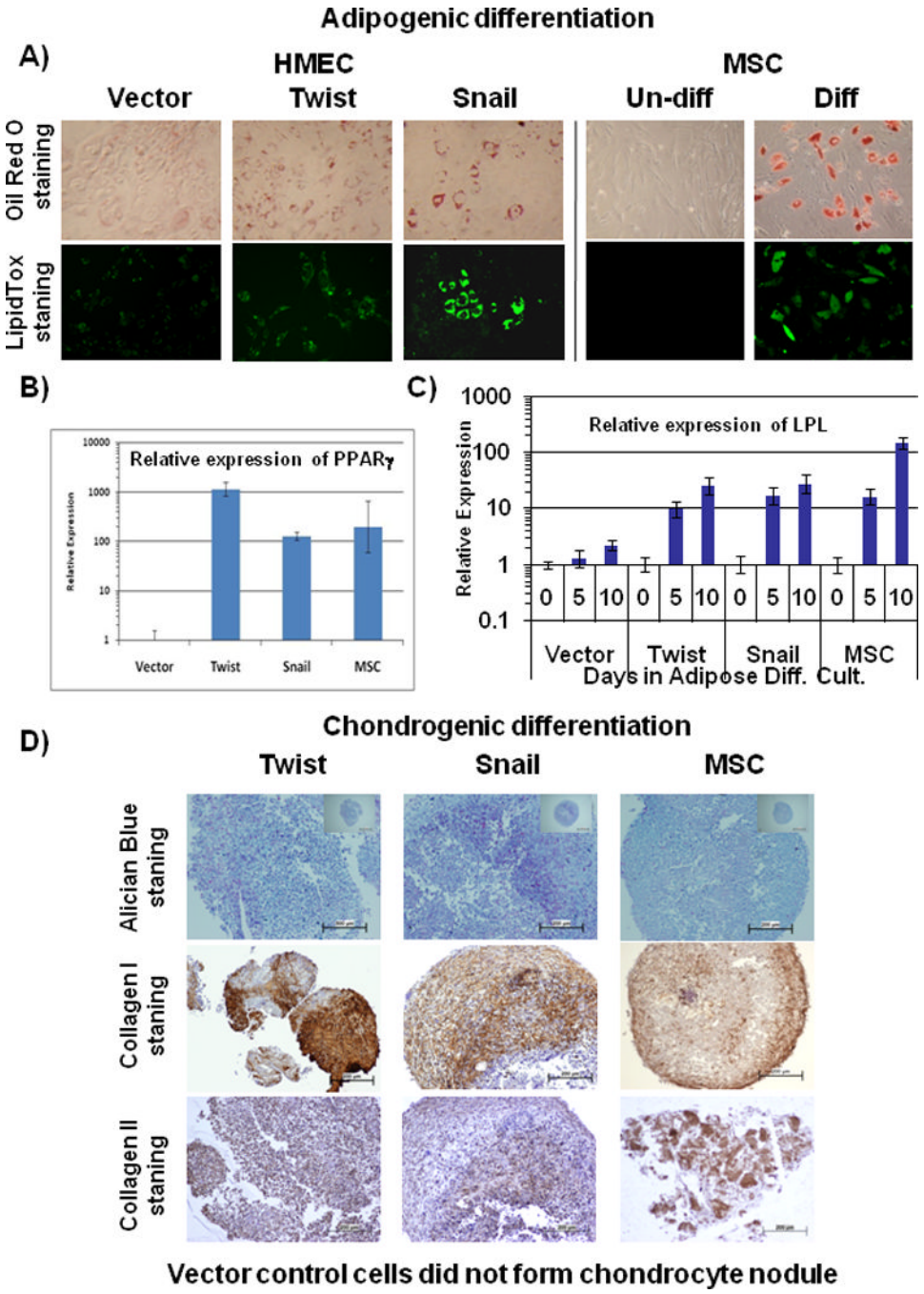

Figure 3.

Adipogenic and chondrogenic differentiation of EMT-derived HMECs and MSCs. **A.** Following adipogenic differentiation, the EMT-derived HMECs and MSCs stained positive with Oil Red O dye (top) and fluorescent LipidTox®, which stains oil droplets (bottom). Conversely, vector control HMECs did not stain using similar treatment (right panel). **B.** Quantitative RT-PCR analysis for the expression of the adipocyte marker PPARγ after 21 days in adipocyte differentiation condition. **C**. Quantitative RT-PCR analysis for the expression of LPL at different time points as indicated in the figure in EMT-derived HMECs, control HMECs and MSCs subjected to adipocyte differentiation. Quantitative RT-

PCR was performed in triplicate (mean +/− SD). **D.** Chondrocytic nodules formed by EMT-derived HMECs or MSCs stained positive with Alcian Blue 8GX (top panel). These sections were counter stained with nuclear fast red solution. Immunohistochemistry was performed on chondrocyte sections using collagen-I antibody (middle panel) and collagen-II (bottom panel). The vector-infected HMECs did not form any chondrocytes nodules under identical conditions.

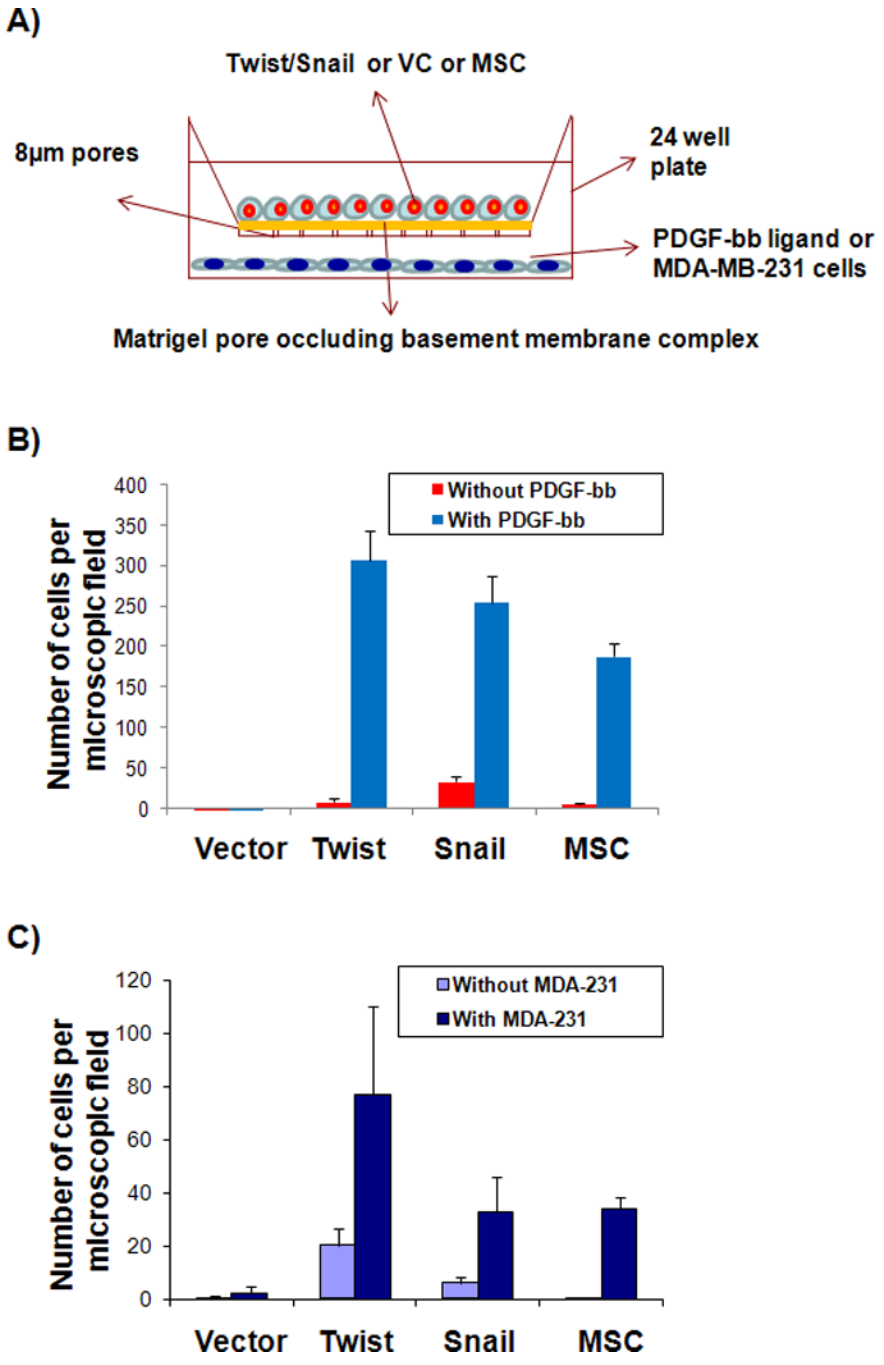

Figure 4.

Matrigel invasion assay to demonstrate migration of EMT-derived cells towards MDA-MB-231 breast cancer cells. (**A**) Three $\times 10^4$ of Twist or Snail or vector alone expressing HMECs or MSCs were incubated in the upper well of the invasion chamber in the presence or absence of PDGF-bb ligand (10ng/ml) (**B**) or MDA-MB-231 cells (**C**) in the bottom well. After 36 hr of incubation, cells that had migrated to the bottom side of the 8 μm membrane were stained and counted as described in methods.

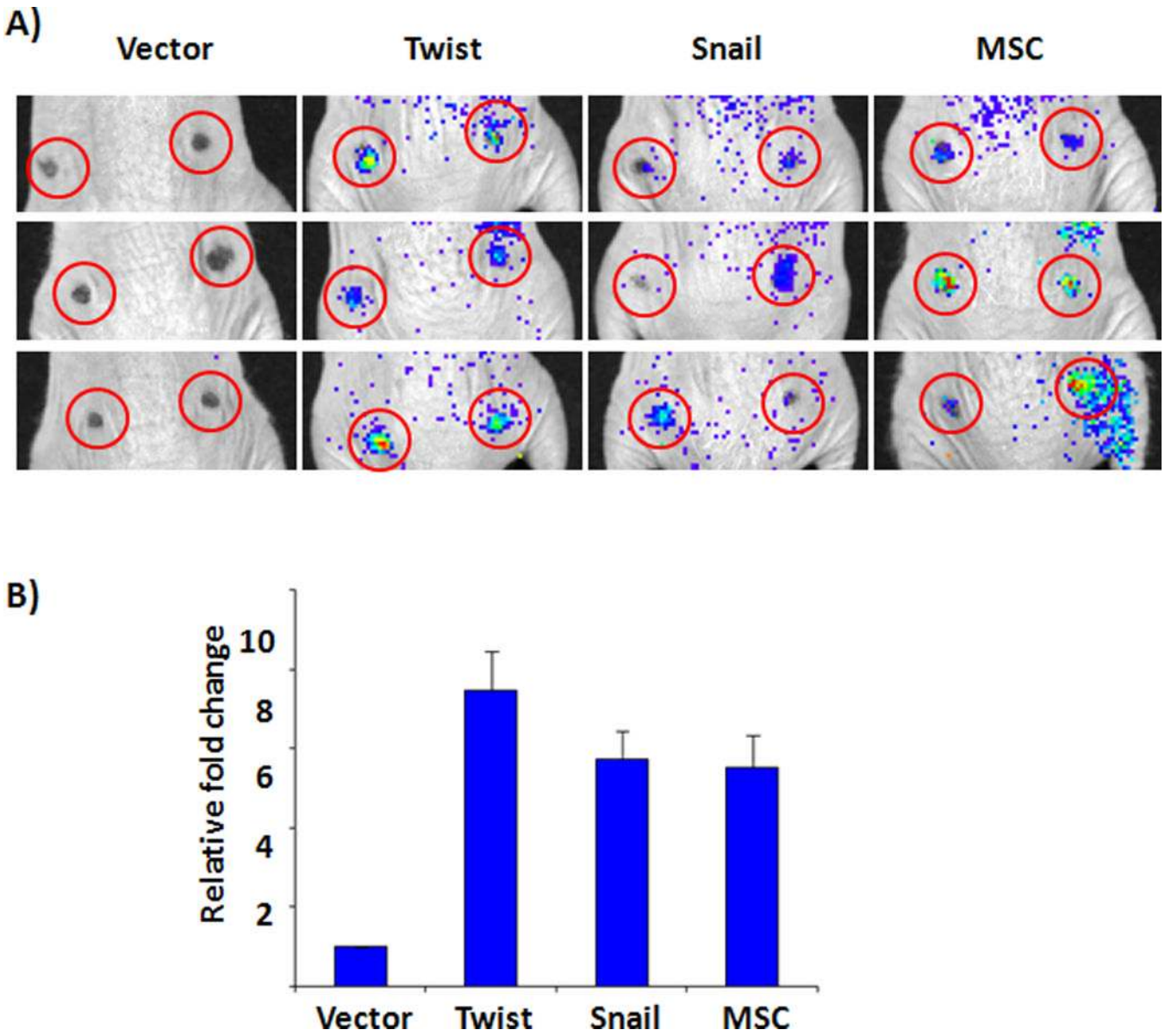

Figure 5.

In vivo wound homing by EMT-derived HMECs and MSCs. (**A**) Bioluminescent imaging of nude mice harboring wounds and injected with 3×10^5 adenoviral firefly luciferase labeled EMT-derived HMECs or MSCs via the tail vein. These experiments were performed in triplicate and repeated three times. (**B**) Quantitative measurement of the relative fold change of bioluminescence. Wound regions were manually drawn and the signal intensity was expressed as photon flux or photons/s/cm^2 (p/s/cm^2) compared to vector control HMECs.

Table 1

Cell surface marker expression of EMT-derived cells and MSCs using flow cytometry. Five × 10^5 HMECs stably expressing Twist, Snail or TGFβ1 and MSCs were incubated with the following antibody conjugates: CD44-APC, CD90-PE, CD105-PE and CD10-PE, CD11c-PE, CD14-PE, CD-24-FITC, CD45-FITC, CD73-PE, CD106-PE, CD140b-PE, CD166-PE. After staining, the cells were analyzed on a LSR-II Flow cytometer. Ten thousand events were acquired for each sample. The flow-cytometric data analysis was performed using FCS Express software. Alternate names and marker distribution is included in a separate column for each marker.

Gene name	Alternate names	Distribution	Twist	Snail	TGF-β	MSC
CD10	Neprilysin	B, T precursors	+	+	+	+
CD11C	Integrin, alpha X	Neutrophils, Dendritic cells	–	–	–	–
CD14	LPS-R	Monocytes, Macrophages	–	–	–	–
CD24	BA-1, HAS	Thymocytes, Erythrocytes	– / low	– / low	– / low	–
CD44	H-CAM	Fibroblasts	+	+	+	+
CD45	PTPRC	Hematopoietic cells	–	–	–	–
CD73	NT5E	Epithelial cells, smooth muscle cells	+	+	+	+
CD90	Thy-1	Fibroblasts, Neurons	+	+	+	+
CD105	Endoglin	Endothelial cells	+	+	+	+
CD106	VCAM-1	Activated endothelial cells	+	+	+	+
CD140b	PDGFRb	Fibroblasts, smooth muscle cells	+	+	+	+
CD166	ALCAM	Neurons, Fibroblats	+	+	+	+